Acta Crystallographica Section F
Structural Biology and Crystallization Communications
ISSN 1744-3091

Crystallization and preliminary X-ray analysis of isopentenyl diphosphate isomerase from *Methanocaldococcus jannaschii*

Takeshi Hoshino,[a] Eriko Nango,[b] Seiki Baba,[a] Tadashi Eguchi[c] and Takashi Kumasaka[a]*

[a]Japan Synchrotron Radiation Research Institute (SPring-8), 1-1-1 Kouto, Sayo, Hyogo 679-5198, Japan, [b]Department of Chemistry, Tokyo Institute of Technology, 2-12-1 O-okayama, Meguro-ku, Tokyo 152-8551, Japan, and [c]Department of Chemistry and Materials Science, Tokyo Institute of Technology, 2-12-1 O-okayama, Meguro-ku, Tokyo 152-8551, Japan

Correspondence e-mail: kumasaka@spring8.or.jp

Received 26 August 2010
Accepted 12 November 2010

Type 2 isopentenyl diphosphate isomerase (IDI-2) is a flavoprotein. Recently, flavin has been proposed to play a role as a general acid–base catalyst with no redox role during the enzyme reaction. To clarify the detailed enzyme reaction mechanism of IDI-2 and the unusual role of flavin, structural analysis of IDI-2 from *Methanocaldococcus jannaschii* (MjIDI) was performed. Recombinant MjIDI was crystallized at 293 K using calcium acetate as a precipitant. The diffraction of the crystal extended to 2.08 Å resolution at 100 K. The crystal belonged to the tetragonal space group *I*422, with unit-cell parameters $a = 126.46$, $c = 120.03$ Å. The presence of one monomer per asymmetric unit gives a crystal volume per protein weight (V_M) of 3.0 Å^3 Da^{-1} and a solvent constant of 59.0% by volume.

1. Introduction

Isoprenoid compounds are ubiquitous in all living species and are diverse in biological function. All isoprenoids are synthesized from the key C_5 units isopentenyl diphosphate (IPP) and dimethylallyl diphosphate (DMAPP). In terpenoid biosynthesis, IPP serves as the elongating C_5 donor and isomerizes to DMAPP. Isopentenyl diphosphate isomerase (IDI; EC 5.3.3.2) is responsible for the isomerization of the carbon–carbon double bond of IPP, forming the potent electrophile DMAPP (Koyama & Ogura, 1999).

IDIs are classified into two distinct types that show no sequence homology to each other. Type 1 IDI (IDI-1) is utilized in most eukaryotes, some bacteria and some halophilic archaea, whereas type 2 IDI (IDI-2) has been reported to be produced by bacteria such as streptomycetes, bacilli and cyanobacteria, trypanosomatids and other archaea (Kuzuyama & Seto, 2003).

IDI-1 is a compact globular α/β protein and requires two divalent metal cations such as Mg^{2+} and Zn^{2+} for activity (Lee & Poulter, 2006). In contrast, IDI-2 is a flavoprotein and requires a divalent cation such as Mg^{2+} for activity. The overall chemical transformation catalyzed by IDI involves a net 1,3 proton-addition/elimination reaction. Interestingly, IDI-2 requires reduced FMN to carry out this redox-neutral isomerization (Bornemann, 2002). IDI-2 reconstituted with cofactor analogues such as 5-deaza-FMN showed no activity, suggesting that FMN plays more than a structural role (Hemmi *et al.*, 2004; Kittleman *et al.*, 2007). Previously, we showed that 3,4-epoxy-3-methylbutyl diphosphate (EIPP), which has been reported to be an IDI-1 mechanism-based inhibitor, can irreversibly inhibit IDI-2 from *Methanocaldococcus janaschii* (MjIDI) and that it covalently binds to the N5 position of reduced FMN instead of to the active-site cysteine of IDI-1 (Hoshino *et al.*, 2006). Furthermore, Rothman and coworkers showed that epoxy, diene and fluorinated substrate analogues give similar results (Rothman *et al.*, 2008). These results indicate that the isomerization mechanism of IDI-2 is a protonation/deprotonation mechanism *via* a carbocation intermediate similar to that of IDI-1 and that the N5 position of reduced FMN plays a key role in the enzyme reaction. This mechanism has also been supported by measurement of the deuterium kinetic isotope effect (Thibodeaux *et*

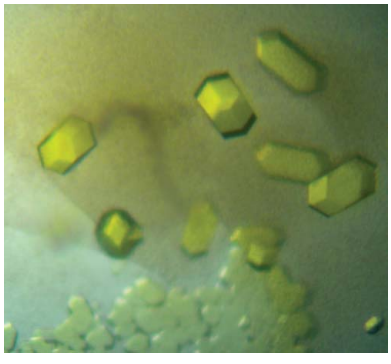

al., 2008) and inhibition study by using alkyne and allene substrate analogues (Sharma *et al.*, 2010).

Crystal structures of IDI-2 from *Bacillus subtilis* (Steinbacher *et al.*, 2003), *Thermus thermophilus* (de Ruyck *et al.*, 2008) and *Sulfolobus shibatae* (Unno *et al.*, 2009) revealed that IDI-2 has a TIM-barrel structure and that its active site is located inside the barrel. From structures of IDI-2 complexed with substrates and the results of kinetic analyses of IDI-2 mutants containing amino-acid substitutions in the active site, Unno and coworkers proposed that the reduced FMN plays the role of an donor/acceptor in the protonation/deprotonation mechanism and that IDI-2 is the first reported flavoenzyme in which reduced flavin acts as a general acid–base catalyst without any redox function. Recently, by synthesizing several FMN analogues and investigating their effects on kinetic parameters, Thiobodeaux and coworkers concluded that the reduced FMN functions as an acid–base catalyst and proposed that the N5 atom of the FMN is one of the acid–base groups that are required for enzymatic turnover (Thibodeaux *et al.*, 2010). However, the other acid–base groups were not identified; therefore, several mechanistic pathways are still being discussed.

We have undertaken the structural analysis of MjIDI and its mechanism-based inhibitor, which will provide detailed information on the mechanism of IDI-2 when combined with the results of a previous kinetic study. In this study, we report the crystallization and preliminary X-ray diffraction analysis of MjIDI.

2. Materials and methods

2.1. Expression and purification

MjIDI is composed of 359 amino acids and its molecular weight is 40 kDa. Its expression in *Escherichia coli* was carried out in accordance with a previously described method (Hoshino *et al.*, 2006). Purification was performed using the previously described method with minor modifications. After heat-treatment of the cell lysate, the supernatant was loaded onto a DEAE Sepharose Fast Flow (GE Healthcare) column previously equilibrated with 20 m*M* HEPES pH 7.5 at a flow rate of 1 ml min^{-1}; the column was eluted with a linear NaCl concentration gradient from 0.2 to 0.6 *M*. The fractions containing MjIDI were combined and concentrated to approximately 2 ml by centrifugation with a Centriprep filter (Amicon Inc.). The concentrate was then loaded onto a 1 ml RESOURCE PHE column (GE Healthcare) previously equilibrated with 20 m*M* HEPES pH 7.5 containing 1 *M* ammonium sulfate and the column was washed with ten bed volumes of the same buffer. The adsorbed proteins were then eluted with 20 m*M* HEPES pH 7.5 containing a linear gradient of ammonium sulfate (1–0 *M*) for 30 min at 1 ml min^{-1}. MjIDI eluted in fractions containing approximately 0.3 *M* ammonium sulfate. The purified enzyme was buffer-exchanged into 50 m*M* HEPES pH 7.5, concentrated to 10 mg ml^{-1} and stored at 193 K.

2.2. Crystallization

Crystallization conditions for MjIDI were initially screened by the sitting-drop vapour-diffusion method at 293 K using the commercially available sparse-matrix screening kits Crystal Screen, Crystal Screen 2, Crystal Screen Cryo, PEG/Ion Screen (Hampton Research), Wizard I, Wizard II, EBS Cryo I, EBS Cryo II (Emerald BioStructures), Structure Screen 1 and Structure Screen 2 (Molecular Dimensions). 1 µl protein solution was mixed with an equal volume of reservoir solution and equilibrated against 100 µl reservoir solution. Layered and stacked crystals appeared using EBS Cryo II condition No. 33 [45%(*v*/*v*) glycerol, 0.1 *M* sodium cacodylate pH 6.5 and 0.2 *M* calcium acetate]. Crystals that diffracted well were obtained using a reservoir consisting of 0.6 *M* calcium acetate and 50 m*M* HEPES pH 7.5 and grew to maximum dimensions of approximately 0.10 × 0.05 × 0.05 mm in 1 d (Fig. 1).

2.3. X-ray diffraction study

Crystals were soaked for a few seconds in a solution consisting of 0.6 *M* calcium acetate and 25%(*w*/*v*) glycerol. The crystal was mounted in a cryoloop and flash-cooled in a liquid-nitrogen stream at 100 K. X-ray diffraction data were collected from MjIDI crystals on beamline BL38B1 at SPring-8 using an ADSC Quantum 210 CCD detector system (ADSC, California, USA). Data collection was performed at a wavelength of 1.0 Å with a total oscillation range of

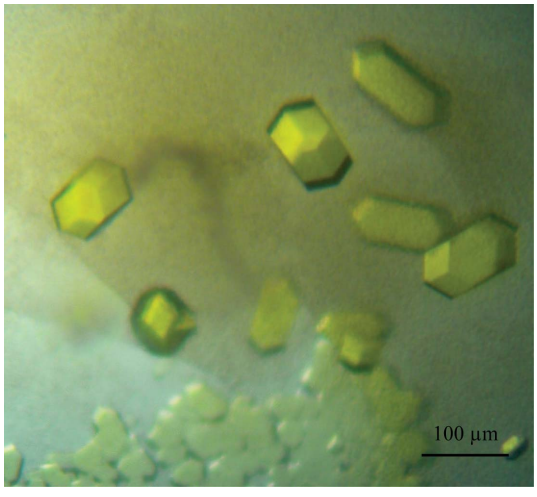

Figure 1
Typical appearance of crystals in hanging drops. The maximum dimensions of the crystals are approximately 0.1 × 0.05 × 0.05 mm.

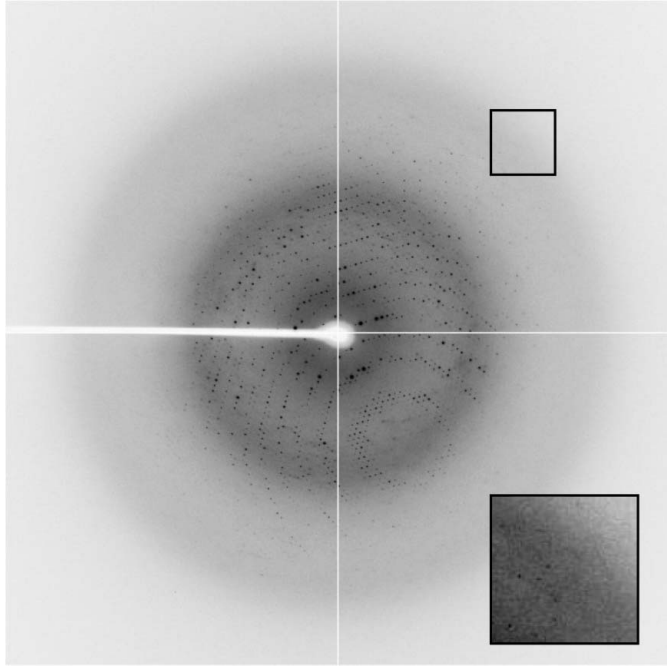

Figure 2
Diffraction pattern of an MjIDI crystal. An enlarged image of the area around 2.08 Å resolution is shown.

Table 1
Data-collection and diffraction data statistics.

Values in parentheses are for the highest resolution shell.

X-ray source	SPring-8 BL38B1
Detector	ADSC Quantum 210
Wavelength (Å)	1.0000
Crystal-to-detector distance (mm)	150
Oscillation angle (°)	0.5
Total oscillation range (°)	100
Space group	*I*422
Unit-cell parameters (Å)	a = 126.46, c = 120.03
Resolution (Å)	35.00–2.08 (2.15–2.08)
Multiplicity	7.9 (7.8)
Completeness (%)	99.8 (100)
$R_{\rm merge}$† (%)	6.7 (42.6)
$\langle I/\sigma(I)\rangle$	34.6 (6.2)

† $R_{\rm merge} = \sum_{hkl}\sum_i |I_i(hkl) - \langle I(hkl)\rangle| / \sum_{hkl}\sum_i I_i(hkl)$, where $I_i(hkl)$ is the intensity of the ith observation and $\langle I(hkl)\rangle$ is the mean intensity of reflection hkl.

100°. Each diffraction image was obtained with an oscillation angle of 0.5° and an exposure time of 5.0 s. The crystal-to-detector distance was set to 150 mm. The data were integrated and scaled using the *HKL*-2000 program package (Otwinowski & Minor, 1997).

3. Results

Single crystals of recombinant MjIDI were obtained by the sparse-matrix method and were optimized to produce single crystals that were suitable for X-ray analysis. Crystals grew to maximum dimensions of 0.1 × 0.05 × 0.05 mm (Fig. 1). X-ray diffraction data for MjIDI were collected to a resolution of 2.08 Å from flash-cooled crystals on the BL38B1 beamline at SPring-8 (Fig. 2). From the diffraction data collected, the space group was determined to be tetragonal *I*422, with unit-cell parameters a = 126.46, c = 120.03 Å. The number of molecules in the asymmetric unit was estimated from the Matthews probability (Kantardjieff & Rupp, 2003). The highest probability (0.99) was obtained for one monomer in the asymmetric unit; the estimated Matthews coefficient was 3.0 Å^3 Da^{-1}, corresponding to a solvent content of 59.0%(*v*/*v*). Scaling and merging of the crystallographic data resulted in an overall $R_{\rm merge}$ of 6.7%. Complete data-collection statistics are shown in Table 1.

The structure was solved by the molecular-replacement method using the *MOLREP* program (Vagin & Teplyakov, 2010) in the *CCP*4 suite (Collaborative Computational Project, Number 4, 1994) with the rigid-body refinement option. X-ray diffraction data from 20 to 2.3 Å resolution were used in this step. The 2.0 Å resolution X-ray structure of monomer *A* of substrate-free isopentenyl diphosphate isomerase from *S. shibatae* (PDB code 2zru; Unno *et al.*, 2009) was used as a search model; the sequence homology between the target protein and the model was 42%, which is higher than those for the other structurally known IDI-2s (*i.e.* those from *B. subtilis* and *T. thermophilus*, which have 28 and 29% sequence homology, respectively). Water molecules and other ions were removed from the model. The model was subsequently subjected to rigid-body refinement in *REFMAC*5 (Murshudov *et al.*, 1997) within the *CCP*4 package, giving an *R* factor of 36.2%. Further model building and restrained refinement are currently in progress.

References

Bornemann, S. (2002). *Nat. Prod. Rep.* **19**, 761–772.
Collaborative Computational Project, Number 4 (1994). *Acta Cryst.* D**50**, 760–763.
Hemmi, H., Ikeda, Y., Yamashita, S., Nakayama, T. & Nishino, T. (2004). *Biochem. Biophys. Res. Commun.* **322**, 905–910.
Hoshino, T., Tamegai, H., Kakinuma, K. & Eguchi, T. (2006). *Bioorg. Med. Chem.* **14**, 6555–6559.
Kantardjieff, K. A. & Rupp, B. (2003). *Protein Sci.* **12**, 1865–1871.
Kittleman, W., Thibodeaux, C. J., Liu, Y., Zhang, H. & Liu, H. (2007). *Biochemistry*, **46**, 8401–8413.
Koyama, T. & Ogura, K. (1999). *Comprehensive Natural Products Chemistry*, edited by D. E. Cane, pp. 69–96. Oxford: Elsevier.
Kuzuyama, T. & Seto, H. (2003). *Nat. Prod. Rep.* **20**, 171–183.
Lee, S. & Poulter, C. D. (2006). *J. Am. Chem. Soc.* **128**, 11545–11550.
Murshudov, G. N., Vagin, A. A. & Dodson, E. J. (1997). *Acta Cryst.* D**53**, 240–255.
Otwinowski, Z. & Minor, W. (1997). *Methods Enzymol.* **276**, 307–326.
Rothman, S. C., Johnston, J. B., Lee, S., Walker, J. R. & Poulter, C. D. (2008). *J. Am. Chem. Soc.* **130**, 4906–4913.
Ruyck, J. de, Pouyez, J., Rothman, S. C., Poulter, D. & Wouters, J. (2008). *Biochemistry*, **47**, 9051–9053.
Sharma, N. K., Pan, J.-J. & Poulter, C. D. (2010). *Biochemistry*, **49**, 6228–6233.
Steinbacher, S., Kaiser, J., Gerhardt, S., Eisenreich, W., Huber, R., Bacher, A. & Rohdich, F. (2003). *J. Mol. Biol.* **329**, 973–982.
Thibodeaux, C. J., Chang, W. & Liu, H. (2010). *J. Am. Chem. Soc.* **132**, 9994–9996.
Thibodeaux, C. J., Mansoorabadi, S. O., Kittleman, W., Chang, W. & Liu, H. (2008). *Biochemistry*, **47**, 2547–2558.
Unno, H., Yamashita, S., Ikeda, Y., Sekiguchi, S. Y., Yoshida, N., Yoshimura, T., Kusunoki, M., Nakayama, T., Nishino, T. & Hemmi, H. (2009). *J. Biol. Chem.* **284**, 9160–9167.
Vagin, A. & Teplyakov, A. (2010). *Acta Cryst.* D**66**, 22–25.